Perchlorate removal in aqueous solutions using periodic mesoporous organosilicas (PMOs) functionalized with quaternary ammonium groups

Sang Don Lee*, Byunghwan Lee*,†, and Kwang-Ho Choo**

*Department of Chemical System Engineering, Keimyung University, 2800 Dalgubeoldaero, Dalseo-gu, Daegu 704-701, Korea
**Department of Environmental Engineering, Kyungpook National University, 1370 Sankyeok-dong, Buk-gu, Daegu 702-701, Korea

Abstract−Perchlorate anion (ClO_4^-) in water has become an environmental issue of concern because it can impair proper functioning of the thyroid gland. For the removal of perchlorate anions from water, adsorption using anion-exchange resins has been generally used as the most suitable method. In this work, we prepared periodic mesoporous organosilica materials (PMOs) functionalized with quaternary ammonium ligands, and used them for the removal of perchlorate anions from aqueous solutions. The physical and chemical properties of prepared samples were measured using nitrogen adsorption-desorption measurement, elemental analyses, X-ray diffractometer, and infrared spectrometer. We also investigated equilibrium isotherms for the measurement of adsorption capacities and kinetic performance of the prepared samples.

Key words: Perchlorate, Periodic Mesoporous Organosilica Materials (PMOs), Quaternary Ammonium Ligands, Anion-exchange Resin

INTRODUCTION

The negatively charged perchlorate ion (ClO_4^-) is composed of one chlorine atom surrounded by four oxygen atoms. Recently perchlorate in water became one of the environmental issues because it can impair proper functioning of the thyroid gland [1,2]. Perchlorate anion salts such as ammonium, potassium, or sodium perchlorate are very soluble in water, and the anions are kinetically inert to reduction and have little tendency to adsorb to mineral or organic surfaces. Therefore, the anions persist in groundwater, and the mobility in surface or groundwater is very high, finally resulting in the concentration in organisms. Compounds containing perchlorate include the oxidant in solid rocket fuel as well as that in fireworks, military ordnance, flares, airbags, and other applications where an energetic oxidant is required. A report on the occurrence of perchlorate in drinking water by the American Water Works Association indicates that perchlorate contamination is a national problem with significant concentrations being found in 26 states and Puerto Rico [2]. A very high concentration of perchlorate (2,225 ppb), which was as 91 times as the USEPA's maximum contaminant level (24.5 ppb), was also reported in Nakdong river, Korea [3].

To separate and remove the perchlorate anions from aqueous solutions, a biological or physical adsorption process has been generally used [4]. For the treatment of perchlorate anions of low concentrations, adsorption processes using anion-exchange resins have been generally used as the most suitable method [4-7]. Especially, resins functionalized with quaternary ammonium groups have been used in various adsorption processes, and have shown high adsorption efficiencies [8-10]. However, these organic anion-exchange resins show some drawbacks due to the characteristics of organic materi-

als: thermal/chemical instability, low surface area, hydrophobicity of polymer matrix, and swelling or deformation in contact with solvents. To overcome these drawbacks, organic/inorganic hybrid anion-exchange resins have been synthesized and widely used to remove anions from wastewater [11,12].

Mesoporous materials have been used as supports for the syntheses of organic/inorganic hybrid anion-exchange resins because they have good mass transfer characteristics due to the uniform pore structures [13-15]. Amine-functionalized mesoporous materials [16], mesoporous materials containing metals, metal cations, or metal oxides [17-21], and mesoporous alumina [22] have been prepared and used for the separation of arsenate, chromate, phosphate, or cesium from aqueous solutions. Mesoporous materials functionalized with quaternary ammonium groups have been synthesized and used to remove anions from aqueous solutions [11,23]. We have also prepared organic/inorganic hybrid anion-exchange resins using mesoporous materials functionalized with quaternary ammonium groups via co-condensation method, and used them for the adsorption of perrhenate anions, which is a surrogate of perchlorate, from aqueous solutions. The relations between the hydrophobicities of prepared mesoporous resins and the adsorption properties were examined systematically [12]. We demonstrated that the surfactant, which was used as a template for the synthesis of mesoporous materials, had an adsorption affinity for perrhenate anions [24]. We also synthesized hybrid nanoporous beads using the prepared powder samples and Na-alginate solutions for the use in the fixed-bed column applications [25].

From the beginning, periodic mesoporous organosilica materials (PMOs) [26,27], PMO-based adsorbents were developed and used for the adsorption of metal ions and organic pollutants by the incorporation of the functional ligands into the PMOs or the use of the intrinsic functionality of the bridged polysilsesquioxane [28]. Some literatures indicate that the adsorption capacity of bulky anions such

as perchlorate may depend on the hydrophobicity of the anion-exchange resins used, and the bulky anions can be adsorbed on the hydrophobic sorbents preferentially [29]. Although some anion-adsorption studies have been performed using PMO-based anion-exchange resins to increase the surface hydrophobicity including ours [12,30], to our knowledge no PMO-based anion-exchange resins have been prepared as support hosts for the removal of perchlorate anions from aqueous solutions. Here we now prepared two types of PMOs containing ethane-bridge (PME) and phenyl-bridge (PMP), and used them for the removal of perchlorate anions from aqueous solutions.

MATERIALS AND METHODS

1. Reagents

Poly(ethylene glycol)-block-poly(propylene glycol)-block-poly(ethylene glycol) (Pluronic P-123, $EO_{20}PO_{70}EO_{20}$, Aldrich), 1,2-bis(trimethoxysilyl)ethane (BTME, 96%, Aldrich), 1,4-bis(triethoxysilyl)benzene (BTEB, 96%, Aldrich), hydrochloric acid (HCl, 37%, Aldrich), ethanol (≥99.5%, Aldrich), N-((trimethoxysilyl)propyl)-N,N,N-trimethylammonium chloride (TSPMC, 50% in methanol, Gelest), N-((trimethoxysilyl)propyl)-N,N,N-tri-n-butylammonium chloride (TSPBC, 50% in methanol, Gelest), and sodium perchlorate (NaClO₄, ≥98.0%, Aldrich) were used as received without further purification.

2. Syntheses and Characterizations

PMOs were synthesized according to the literature [27,31]. For the synthesis of ethane-bridged PMO (PME), 2.1 g of P-123 was dissolved in the mixture of 82.9 ml of water and 1.14 ml of concentrated HCl at 50 °C. Then 2.61 ml of BTME was slowly added to the solution at 40 °C under vigorous stirring. The final molar composition of reactants was 0.035 P-123 : 1.34 HCl : 444 H_2O : 1 BTME. After 24 h, the solid was filtered and washed with enormous amounts of distilled water. The resulting powders were refluxed with acidic ethanol for 8 h, and washed again with enormous amounts of distilled water and ethanol. After drying in oven at 90 °C for 3 h and drying in vacuum at 105 °C for 5 h, PME was obtained. Phenyl-bridged PMO (PMP) was also prepared using the similar procedure using BTEB as an organosilica precursor instead of BTME.

To prepare PME functionalized with methylammonium ligands (PME-M), 1 ml of TSPMC was dropped to the mixture of 1 g of PME and 100 ml of toluene, and the mixture was vigorously stirred at 50 °C for 24 h. The solid was filtered and washed with toluene. The resulting powders were dried in oven at 90 °C for 3 h, dried in vacuum at 115 °C for 5 h, and then PME-M was obtained. PME functionalized with butylammonium ligands (PME-B) was prepared by the similar procedure using TSPBC as a functional ligand instead of TSPMC. PMP functionalized with methylammonium ligands (PMP-M) and butylammonium ligands (PMP-B) were also prepared by the similar procedures using PMP as a support host instead of PME.

N₂ adsorption/desorption measurements (ASAP 2010, Micromeritics, USA) were performed at 77 K. The surface areas of the prepared samples were determined by BET method, and the pore size distribution was obtained from BJH adsorption data. X-ray diffraction (XRD) patterns were obtained at 40 kV and 25 mA using CuK$_\alpha$ radiation (wavelength=0.154 nm) on a powder X-ray diffractometer (X'pert APD, Philips). Fourier transform infrared (FTIR, Research2,

ATI Mattson, US) spectroscopy was used to examine the existence of organic groups in the prepared samples. A CHNS analyzer (Flash 2000, ThermoFisher) was used to measure the amount of functional groups in the samples.

3. Anion Adsorption

Adsorption isotherms were obtained via batch equilibrium experiments. Anion-exchange resin of 0.1 g was mixed with 10 ml of aqueous solutions containing perchlorates of which concentrations ranged from 20 mg/l to 2,924 mg/l. The mixtures were sonicated at 45 W for 10 min using ultrasonic machine (KODO, JAC-1505), stirred at room temperature for 24 h, and then filtered using 0.45 μm membrane. The concentration of perchlorate was measured using ion chromatography (IC, Dionex, DX-120) equipped with an Ion-Pac®AS16 analytical column. The sample size was 2.0 ml, the flow rate was 1.0 ml/min, and the eluent was 35 mM sodium hydroxide. The amount of perchlorate adsorbed onto the anion-exchange resin was calculated by a mass balance relationship:

$$q_e = (C_0 - C_e)V/m \tag{1}$$

where q_e is the amount of adsorbed perchlorate on anion-exchange resin at equilibrium (mg/g), C_0 the initial perchlorate concentration of aqueous solution (mg/l), C_e the perchlorate concentration in solution at equilibrium (mg/l), V the volume of the solution (l), and m the mass of the adsorbent (g). Langmuir adsorption isotherm was used to model the perchlorate adsorption behavior:

$$q_e = \frac{Q^0 bC_e}{1+bC_e} \tag{2}$$

where Q^0 is the maximum adsorption capacity (mg/g) and b a constant related to the affinity of the binding sites (l/mg).

To measure kinetic uptake of perchlorate onto the prepared materials, semi-batch adsorption experiments were performed. Sample powder of 0.1 g was mixed with 1 l of 0.1 mmol/l perchlorate aqueous solution. The suspended samples of 5 ml were taken at various time intervals under the vigorous stirring of the solution. The samples were filtered using a 0.45 μm pore filter unit, and the perchlorate concentration of the filtrate was measured using an IC system. Pseudo-second-order equation was used to model the kinetic data of perchlorate adsorption on the prepared anion-exchange resins [23,24]:

$$\frac{dq_t}{dt} = k_2(q_e - q_t)^2 \tag{3}$$

where k_2 is the rate constant of pseudo-second-order adsorption (g/mg·min) and q_t the amount of adsorbed perchlorate on the anion-exchange resin at time t (mg/g). The integrated form of Eq. (3) is expressed as:

$$\frac{t}{q_t} = \frac{1}{k_2 q_e^2} + \frac{1}{q_e}t \tag{4}$$

RESULTS AND DISCUSSION

1. Characterization

N₂ adsorption-desorption isotherms of the prepared materials were determined and shown in Fig. 1(a) and Fig. 2(a). All prepared materials showed type IV isotherm classified by IUPAC, which was typi-
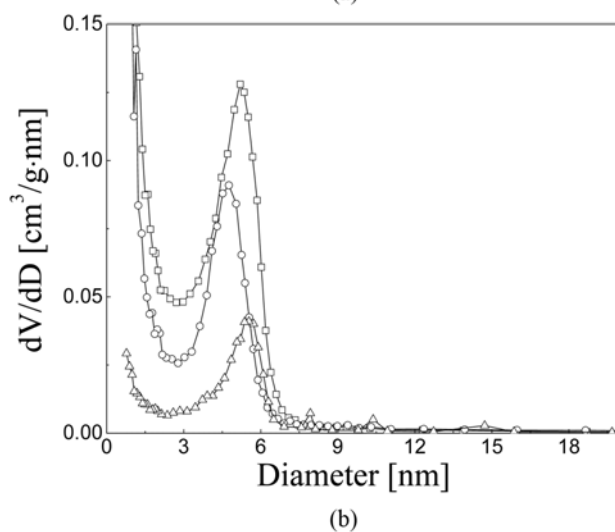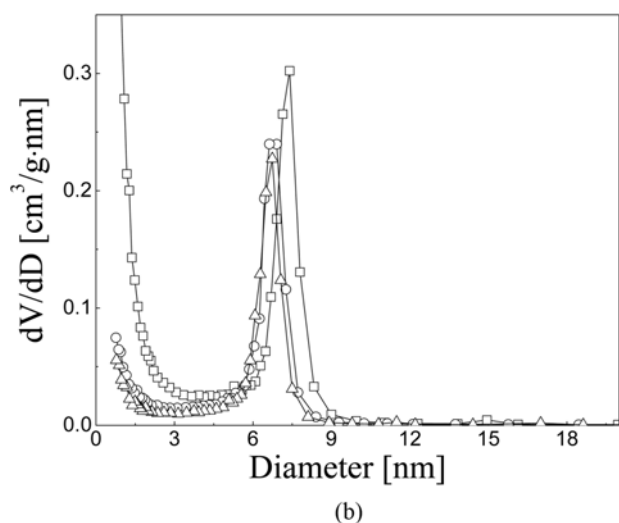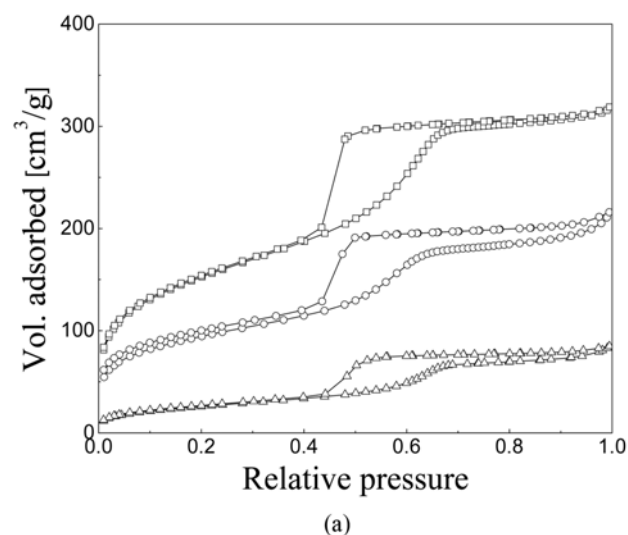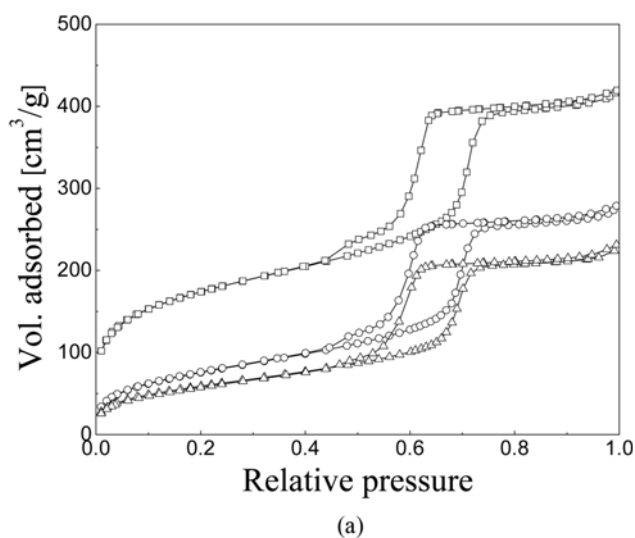
Fig. 1. (a) N_2 adsorption-desorption isotherms and (b) BJH pore size distributions of PME (□), PME-M (○), and PME-B (△).

Fig. 2. (a) N_2 adsorption-desorption isotherms and (b) BJH pore size distributions of PMP (□), PMP-M (○), and PMP-B (△).

cal of mesoporous materials [32]. PME materials exhibited more steep steps in the adsorption curves than PMP materials, indicating that PME materials had narrower and more homogeneous pore size distributions than PMP materials. This result is consistent with the pore size distribution data showing monodisperse peaks in PME materials (Fig. 1(b)), while those of PMP materials show relatively broad distributions (Fig. 2(b)). Table 1 shows the properties of the prepared anion-exchange resins. Among the prepared materials,

Table 1. Properties of the prepared anion-exchange resins: surface area, pore diameter, pore volume, d spacing, relative intensities, and number of functional groups

Sample	Surface area[a] [m²/g]	Pore diameter[b] [nm]	Pore volume[c] [cm³/g]	d_{100} [nm]	I/I_0[d]	N [mmol/g]	N [/nm²]
PME	599	7.4	0.64	10.6	-	-	-
PME-M	282	6.9	0.41	10.8	0.83	0.95	2.03
PME-B	282	6.7	0.35	11.1	0.66	1.11	2.37
PMP	540	5.4	0.48	10.3	-	-	-
PMP-M	331	4.8	0.32	9.9	0.79	1.22	2.22
PMP-B	96	5.7	0.13	10.3	0.51	0.64	4.01

[a]BET surface area

[b]The maximum diameter in BJH adsorption pore size distribution

[c]Single point total pore volume

[d]Relative intensity, I/I_0=(intensity of sample)/(intensity of PME or PMP)
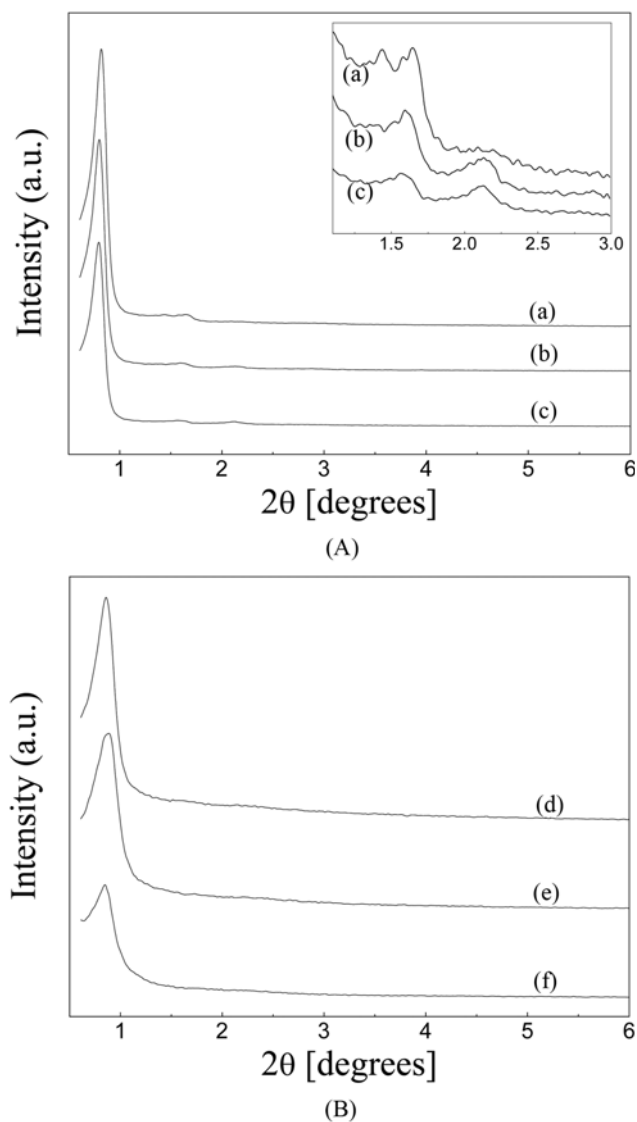
Fig. 3. XRD patterns of PME (a), PME-M (b), PME-B (c), PMP (d), PMP-M (e), and PMP-B (f): The spectra (a), (b), (d), and (e) were shifted up vertically, and the weak reflections of (a), (b), and (c) were 2 times magnified as shown in the inset of (A) for clarity.
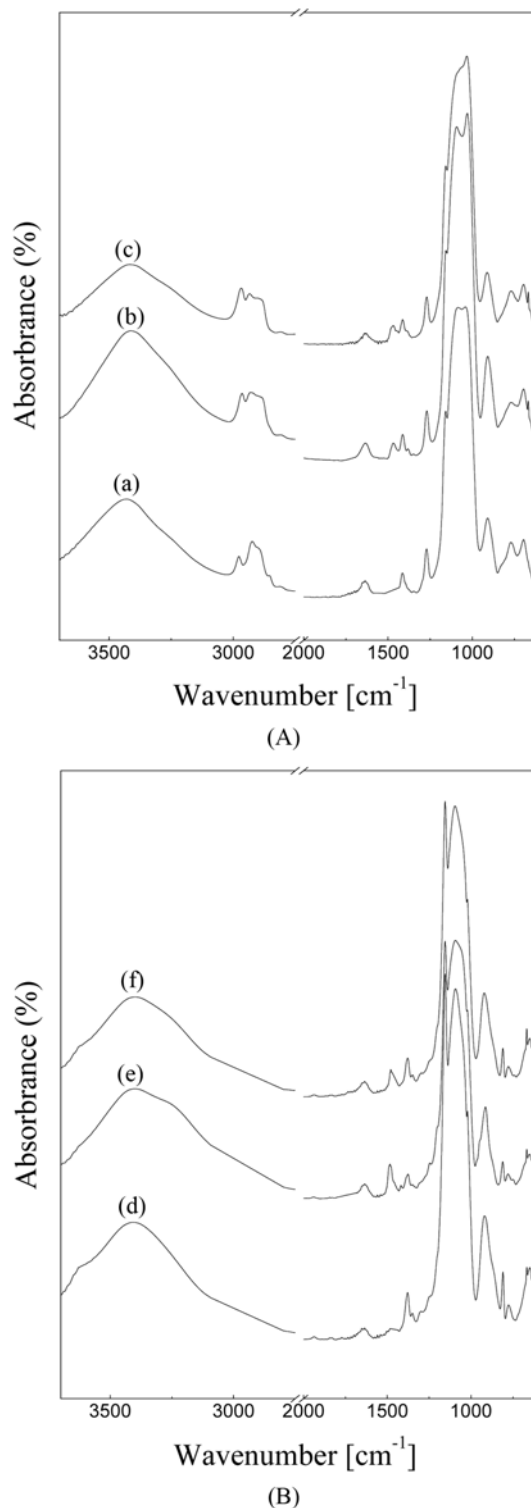

Fig. 4. FTIR spectra of PME (a), PME-M (b), PME-B (c), PMP (d), PMP-M (e), and PMP-B (f): The spectra (b), (c), (e), and (f) were shifted vertically 20%, 30%, 40%, and 60% up respectively for clarity.

PME and PMP showed relatively large surface areas of 599 and 540 m^2/g, respectively. After impregnating the methylammonium ligands (PME-M and PMP-M) or butylammonium ligands (PME-B and PMP-B), the surface areas, pore sizes, and pore volumes decreased due to the incorporation of organic groups onto the mesopores. The decrease was especially significant in PMP-B.

XRD patterns of the prepared materials were obtained and shown in Fig. 3. XRD pattern indicates that PME has a typical hexagonal structure showing one main reflection at 0.83°, and three additional weak reflections at 1.43°, 1.65°, and 2.13° corresponding to the 100, 110, 200, and 210 diffraction planes respectively [32]. Compared with the XRD spectrum of PME, PME-M and PME-B showed lower intensities of the corresponding peaks (Table 1) and the second reflections disappeared (inset of Fig. 3(a)), showing the decrease of the crystallinity due to the functionalization. However, PME-M and

PME-B still had the third and fourth reflections, indicating that the quaternary ammonium functionalized materials still had the hexagonal structures. XRD spectra of PMP materials just showed a main reflection with no additional weak reflections, indicating that the crys-

tallinities of PMP materials were lower than those of PME materials. This is consistent with the results of N_2 adsorption-desorption measurements. PMP-M and PMP-B also exhibited decreased XRD peak intensities due to the impregnation step (Table 1).

Fig. 4 shows the FTIR spectra of the prepared anion-exchange resins. The FTIR spectrum of PME shows a band at 1,636 cm^{-1}, which is attributed to the asymmetric ethylene (C-C) stretching modes. The peaks at 1,270, 1,414, and 2,923 cm^{-1} are attributed to the bridging ethylene C-H vibration and stretching, respectively. The bands at 1,040 and 3,429 cm^{-1} are attributed to Si-O stretching from the siloxane bonds and the Si-OH groups, respectively [33]. In the FTIR spectrum of PMP, the bands at 1,155 and 1,377 cm^{-1} are attributed to Si-C bonds and phenyl groups, respectively [34]. While PME and PMP show no band from 1,490 to 1,460 cm^{-1}, quaternary ammonium-functionalized PME (PME-M or PME-B) and PMP (PMP-M or PMP-B) have extra bands at 1,468 and 1,482 cm^{-1}, respectively. These bands confirm the presence of trimethylammonium or tributylammonium ligands in the samples, implying the successful impregnation of functional groups [24,35].

The results of elemental analyses are shown in Table 1. In the bare PMO materials, nitrogen was not detected, indicating that there were no functional groups in PME and PMP. Considering all functional groups were located on the surface of the PMO materials due to the synthetic procedures via impregnation method, the number of functional groups on the unit surface area was calculated using the results of elemental analyses and BET surface areas of the samples (Table 1). In the previous studies [24,36], the surface densities of functional groups, such as quaternary ammoniums or thiols, ranged from 0.14 to 2.01 nm^{-2}. PME-M, PME-B, and PMP-M showed the comparable values of 2.03, 2.37, and 2.22 nm^{-2}, respectively, indicating that the quaternary ammonium groups were successfully functionalized on the surface of PMO materials. However, PMP-B showed relatively large density of functional groups (4.01 nm^{-2}) due to the small surface area (96 m^2/g). This result implies that the large tributylammonium functional groups might block some mesopores of PMP, resulting in the remarkable reduction of the surface area of PMP-B compared with that of the support material, PMP. This is consistent with the pore size distribution data of PMP-B in Fig. 2(b). Except PMP-B, all the prepared anion-exchange resins showed the reduced pore size compared with the bare PMO materials, and the pore size distributions were shifted a little to the smaller values after the impregnation step. However, the pore size distribution of PMP-B drastically decreased after functionalization, showing the large decrease of the mesopore volumes less than 5 nm. The change of pore structure like this can induce low perchlorate adsorption capability, which will be discussed later.

2. Anion Adsorption

Equilibrium adsorption experiments of perchlorate anions were carried out in single-solute solutions using the prepared anion-exchange resins. PME and PMP with no functional groups showed a little adsorption capabilities for perchlorate anions with adsorption capacities less than 13 mg/g in the experimental concentrations. Compared with PME or PMP, the prepared anion-exchange resins showed larger adsorption capacities for perchlorate anions, indicating that quaternary ammonium functional groups incorporated onto the pore walls had a strong affinity for perchlorate anions. As shown in Table 2 and Fig. 5, the equilibrium adsorption isotherms were well fitted

Table 2. Langmuir isotherm parameters in the adsorption of perchlorate on the prepared anion-exchange resins

Sample	Q^0 [mg/g]	b [L/mg]	R^2	Q_{NA} [mg/m^2]
PME-M	135.1	3.65×10^{-3}	0.9796	0.48
PME-B	142.9	5.96×10^{-3}	0.9957	0.51
PMP-M	135.1	3.47×10^{-3}	0.9757	0.41
PMP-B	106.4	5.53×10^{-3}	0.9906	1.11

Q^0: Maximum adsorption capacity
b: Langmuir constant
R^2: Correlation coefficient
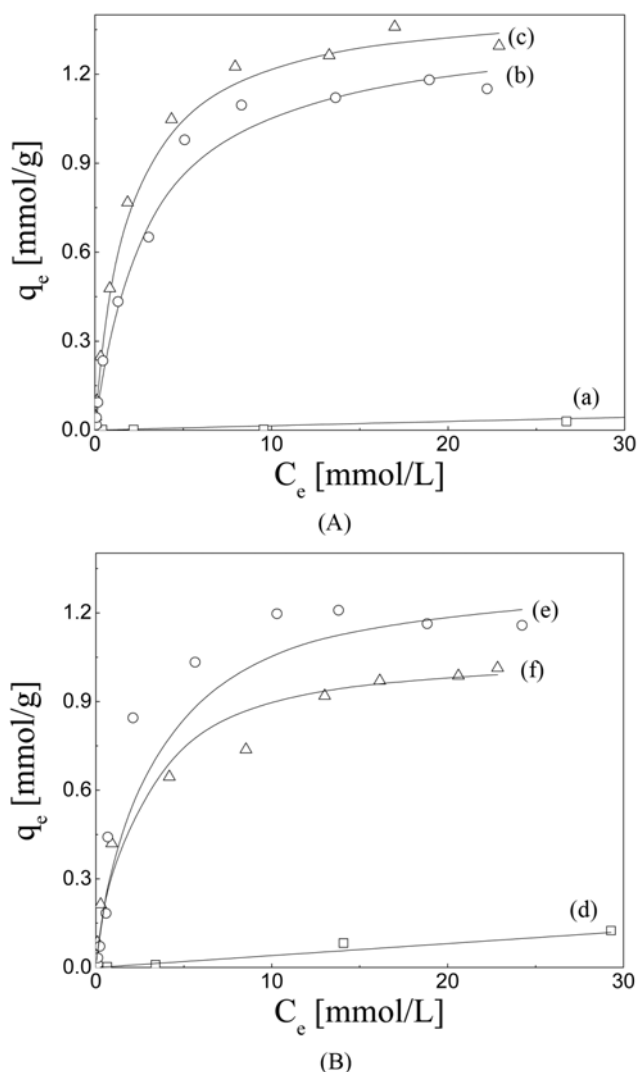Q_{NA}: Normalized adsorption capacity

Fig. 5. Adsorption isotherms of perchlorate on PME (a), PME-M (b), PME-B (c), PMP (d), PMP-M (e), and PMP-B (f): Data were fitted with Langmuir model (solid lines).

with the Langmuir isotherm model, showing the R^2 values over 0.98 for all the prepared anion-exchange resins. Perchlorate adsorption capacities obtained from the Langmuir model were 135.1, 142.9, 135.1, and 106.4 mg/g for PME-M, PME-B, PMP-M, and PMP-B, respectively. The normalized adsorption capacities, Q_{NA}, of per-
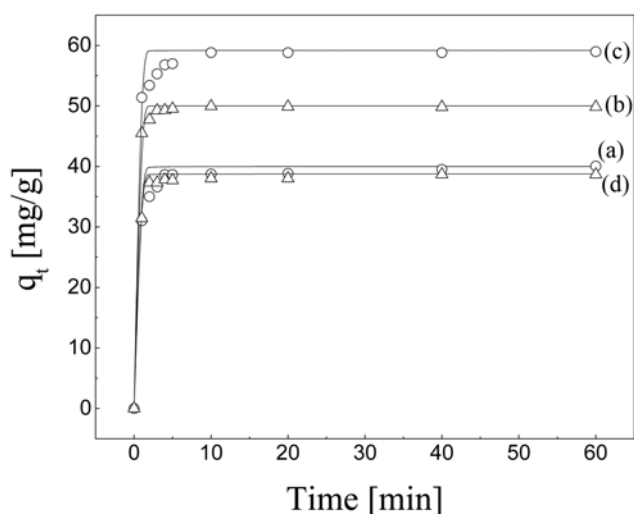
Fig. 6. Time-resolved uptake of perchlorate on PME-M (a), PME-B (b), PMP-M (c), and PMP-B (d), and fitting plots of the perchlorate adsorption kinetics which were obtained using pseudo-second-order kinetic model (solid lines).

chlorate per unit surface area were determined using BET surface area and maximum adsorption capacity obtained from Langmuir isotherm (Table 2). PME-M, PME-B, and PMP-M had relatively similar Q_{NA} values of 0.48, 0.51, and 0.41 mg/m^2, respectively. Q_{NA} of PMP-B (1.11 mg/m^2) was about two-times larger than those of the other anion-exchange resins due to the high density of functional groups. However, it had the smallest adsorption capacity among the anion-exchange resins used because of the small surface area. The low perchlorate adsorption capability of PMP-B may be ascribed to the significant decrease of mesopores as described above.

To determine the kinetic adsorption rate, perchlorate anion adsorption experiments were performed using a semi-batch reactor (Fig. 6). The prepared anion-exchange resins showed fast adsorption rates for perchlorate. The required contact time to reach equilibrium was less than 10 min for all the anion-exchange resins used. These results indicate that the contact time of 24 h was enough for the equilibrium adsorption experiments described in the above section. Adsorption kinetic data were fitted with pseudo-second-order model because it was reported that the pseudo-second-order model showed best correlations with the experimental data in metal adsorption among the kinetic models, including the pseudo-first-order model, pseudo-second-order model, and parabolic diffusion model [24,37]. The fitting plots and the parameters for the model were determined and

Table 3. Adsorption kinetic parameters calculated from pseudo-second-order kinetic model

Sample	$q_{e, exp}$ [mg/g]	$q_{e, cal}$ [mg/g]	k_2 [g/mg·min]	R^2
PME-M	40.1	40.0	3.85	0.9999
PME-B	49.8	50.0	25.0	0.9999
PMP-M	59.0	59.2	7.35	0.9999
PMP-B	38.7	38.8	7.17	0.9999

$q_{e, exp}$: Adsorption capacity measured from experiment
$q_{e, cal}$: Adsorption capacity estimated by the kinetic model
k_2: Rate constant of pseudo-second-order equation

shown in Fig. 6 and Table 3. The R^2 values for this kinetic model were 0.9999 for all the anion-exchange resins used, showing that the adsorption kinetic for the prepared anion-exchange resins followed well the pseudo-second-order model. The adsorption capacity estimated by the kinetic model, $q_{e, cal}$ also coincided well with the experimental data, $q_{e, exp}$ (Table 3). The $q_{e, cal}$ values were smaller than those of the Q^0 values obtained from adsorption isotherms, showing the values from 30% to 44% of the Q^0 values. Generally, the adsorption capacity calculated using pseudo-second-order equation from kinetic data shows smaller value than the adsorption capacity obtained from Langmuir model, which shows the maximum adsorption capacity [25].

In the previous researches, anion-exchange resins based on the mesoporous silica materials were prepared, and those materials showed adsorption capacities for perrhenate anion, which is a surrogate of perchlorate, less than 27 mg/g [24,25]. The larger adsorption capacities of anion-exchange resins prepared in this work might be ascribed to the hydrophobic surfaces of the PMO-based materials, which can be measured using water vapor adsorption [32,38]. These results suggest that the PMO-based anion-exchange resins are good candidates for the removal of perchlorate anions from aqueous solutions.

CONCLUSIONS

We synthesized PMO-based anion-exchange resins and used them for the removal of perchlorate anions from aqueous solutions. The prepared anion-exchange resins showed high perchlorate adsorption capacity of 142.9 mg/g (PME-B). This value is much larger than those of silica-based anion-exchange resins for perrhenate anions in previous studies. The large adsorption capacity might be ascribed to the hydrophobic surfaces of the PMO-based materials. The prepared anion-exchange resins also showed fast adsorption kinetic performances. These results show that the PMO-based anion-exchange resins can be an alternative for the removal of perchlorate anions from water.

ACKNOWLEDGEMENT

REFERENCES

1. R. J. Bull, A. C. Chang, C. F. Cranor, R. C. Shank and R. Trussell, *Perchlorate in drinking water: A science and policy review*, Urban Water Research Center, University of California, Irvine, CA (2004).
2. G. M. Brown and B. Gu, in *Perchlorate: Environmental occurrence, interactions and treatment*, B. Gu and J. D. Coates Eds., Springer, New York (2006).
3. Yonhap News, July 28 (2006).
4. B. E. Logan, *Environ. Sci. Technol.*, **35**, 482A (2001).
5. Z. Xiong, D. Zhao and W. F. Harper Jr., *Ind. Eng. Chem. Res.*, **46**, 9213 (2007).
6. K. Hristovski, P. Westerhoff, T. Möller, P. Sylvester, W. Condit and

H. Mash, *J. Hazard. Mater.*, **152**, 397 (2008).

7. I.-H. Yoon, X. Meng, C. Wang, K.-W. Kim, S. Bang, E. Choe and L. Lippincott, *J. Hazard. Mater.*, **164**, 87 (2009).

8. B. Gu, Y.-K. Ku and G. M. Brown, *Federal Facilities Environ. J.*, Spring, 75 (2003).

9. B. Gu, Y.-K. Ku and G. M. Brown, *Environ. Sci. Technol.*, **39**, 901 (2005).

10. B. Gu, G. M. Brown and C.-C. Chiang, *Environ. Sci. Technol.*, **41**, 6277 (2007).

11. Y. H. Ju, O. F. Webb, S. Dai, J. S. Lin and C. E. Barnes, *Ind. Eng. Chem. Res.*, **39**, 550 (2000).

12. B. Lee, L.-L. Bao, H.-J. Im, S. Dai, E. W. Hagaman and J. S. Lin, *Langmuir*, **19**, 4246 (2003).

13. C. T. Kresge, M. E. Leonowicz, W. J. Roth, J. C. Vartuli and J. S. Beck, *Nature*, **359**, 710 (1992).

14. P. T. Tanev and T. J. Pinnavaia, *Science*, **267**, 865 (1995).

15. D. Zhao, J. Feng, Q. Huo, N. Melosh, G. H. Fredrickson, B. F. Chmelka and G. D. Stucky, *Science*, **279**, 548 (1998).

16. H. Yoshitake, T. Yokoi and T. Tatsumi, *Chem. Mater.*, **14**, 4603 (2002).

17. G. E. Fryxell, J. Liu, T. A. Hauser, Z. Nie, K. F. Ferris, S. Mattigod, M. Gong and R. T. Hallen, *Chem. Mater.*, **11**, 2148 (1999).

18. Y. Lin, G. E. Fryxell, H. Wu and M. Engelhard, *Environ. Sci. Technol.*, **35**, 3962 (2001).

19. H. Yoshitake, T. Yokoi and T. Tatsumi, *Chem. Mater.*, **15**, 1713 (2003).

20. M. Jang, E. W. Shin, J. K. Park and S. I. Choi, *Environ. Sci. Technol.*, **37**, 5062 (2003).

21. E. W. Shin, J. S. Han, M. Jang, S.-H. Min, J. K. Park and R. M. Rowell, *Environ. Sci. Technol.*, **38**, 912 (2004).

22. Y. Kim, C. Kim, I. Choi, S. Rengaraj and J. Yi, *Environ. Sci. Technol.*, **38**, 924 (2004).

23. T.-H. Kim, M. Jang and J. K. Park, *Micropor. Mesopor. Mater.*, **108**, 22 (2008).

24. B. Lee, Y.-S. Chung and C. Park, *Korean Chem. Eng. Res.*, **46**, 436 (2008).

25. Y.-S. Chung, B. Lee, K.-H. Choo and S.-J. Choi, *J. Ind. Eng. Chem.*, **17**, 114 (2011).

26. S. Inagaki, S. Guan, T. Ohsuna and O. Terasaki, *Nature*, **416**, 304 (2002).

27. Y. Goto and S. Inagaki, *Chem. Commun.*, 2410 (2002).

28. M. C. Burleigh, M. A. Markowitz, M. S. Spector and B. P. Gaber, *Environ. Sci. Technol.*, **36**, 2515 (2002).

29. M. E. Barr, G. D. Jarvinen, E. W. Moody, R. Vaughn, L. A. Silks and R. A. Bartsch, *Sep. Sci. Technol.*, **37**, 1065 (2002).

30. B. Lee, H.-J. Im, H. Luo, E. W. Hagaman and S. Dai, *Langmuir*, **21**, 5372 (2005).

31. S. Z. Qiao, C. Z. Yu, Q. H. Hu, Y. G. Jin, X. F. Zhou, X. S. Zhao and G. Q. Lu, *Micropor. Mesopor. Mater.*, **91**, 59 (2006).

32. Y.-H. Kim, B. Lee, K.-H. Choo and S.-J. Choi, *Micropor. Mesopor. Mater.*, **138**, 184 (2011).

33. N. Hao, H. Wang, P. A. Webley and D. Zhao, *Micropor. Mesopor. Mater.*, **132**, 543 (2010).

34. S. L. Burkett, S. D. Sims and S. Mann, *Chem. Commun.*, 1367 (1996).

35. G. Socrates, *Infrared and raman characteristic group frequencies*, 3rd Ed., Wiley, Chichester (2001).

36. Y. Kim, B. Lee, Y. S. Cho and J. Yi, *Korean Chem. Eng. Res.*, **39**, 228 (2001).

37. H. S. Choi, D. G. Lee, G. J. Cho, C. Y. Lee, J. S. Chung, I.-K. Yoo and E. W. Shin, *Korean Chem. Eng. Res.*, **44**, 172 (2006).

38. B. Lee, Y. Kim, H. Lee and J. Yi, *Micropor. Mesopor. Mater.*, **50**, 77 (2001).